

Magnetoconductivity due to Quantum Interference in Strongly Underdoped $YBa_2Cu_3O_x$

E. Cimpoiasu, G. A. Levin, and C. C. Almasan
Department of Physics, Kent State University, Kent OH 44242

Hong Zheng and B. W. Veal
Materials Science Division, Argonne National Laboratory, Argonne, IL 60439

We report magnetoconductivity measurements on $YBa_2Cu_3O_x$ ($x = 6.25$ and 6.36) single crystals. Our main result is that both the in-plane $\Delta\sigma_{ab}$ and out-of-plane $\Delta\sigma_c$ magnetoconductivities exhibit the field dependence characteristic of "two-dimensional" quantum interference in applied magnetic fields $H\parallel c$. Namely, $\Delta\sigma_{c,ab} \propto \ln H/H_0 > 0$, with $\Delta\sigma_c/\sigma_c$ substantially greater than $\Delta\sigma_{ab}/\sigma_{ab}$. We interpret this result as an evidence of interlayer incoherence in these crystals, so that the phase-coherent trajectories are mostly confined to one bilayer.

(November 1, 2018)

I. INTRODUCTION

Understanding the anomalous features of the in-plane and out-of-plane normal state transport in layered cuprates remains a challenge. Among the properties of the resistivity tensor $\{\rho_c, \rho_{ab}\}$ that are some of the most unusual from the point of view of the conventional Fermi liquid theory are strongly temperature dependent anisotropy ρ_c/ρ_{ab} and coexistence of metallic $\rho_{ab}(T)$ and nonmetallic $\rho_c(T)$ over extended temperature and doping ranges. It has been suggested that these anomalies of the out-of-plane transport are the result of interlayer incoherence [1,2]. This means that the phase coherent trajectories along which the single electrons maintain their phase memory are all confined to a single bilayer because the interbilayer transitions lead to dephasing of still unknown origin. An experimental confirmation of c-axis incoherence was provided by optical measurements [3].

The suggestion of interlayer incoherence in the normal state of the cuprates, however, is not fully accepted. There are alternative models of the out-of-plane transport that do not involve interlayer incoherence [4,5]. The phase coherent trajectories in such models are three dimensional and extend over many unit cells in both the in- and out-of-plane directions.

Magnetoeffects due to quantum interference allow, in principle, the determination of the dimensionality of the phase coherence. Magnetoconductivity arises in relatively small magnetic fields due to contributions of the self-intersecting phase coherent trajectories along which the loops can be traversed in two different directions [6,7,8]. The magnitude and field dependence of magnetoconductivity are determined by the probability of a trajectory to form a loop of a given area. If the phase-coherent trajectories are two-dimensional 2D, they are substantially more likely to form large loops than three-dimensional 3D ones. This results in a more pronounced effect, observable at higher temperatures. The field de-

pendence of magnetoconductivity is also different in these two cases; namely, 2D trajectories lead to $\Delta\sigma \propto \ln H$, while 3D trajectories lead to $\Delta\sigma \propto H^{1/2}$.

Here we present magnetoresistivities of two strongly underdoped $YBa_2Cu_3O_{6.25}$ and $YBa_2Cu_3O_{6.36}$ single crystals. Our results can be summarized as follows: Both components $\Delta\rho_c/\rho_c$ and $\Delta\rho_{ab}/\rho_{ab}$ of the magnetoresistivity tensor reveal the presence of two different conduction mechanisms in magnetic fields $H\parallel c$. (1) In low fields, the magnetoresistivities are negative and have a logarithmic field dependence over about a decade (at the lowest accessible temperature). This behavior represent the main focus of this paper. What distinguishes these results from traditional experiments on ultrathin films and other 2D systems [6,9], is that the out-of-plane magnetoresistivity has the logarithmic field dependence and is substantially larger than the in-plane magnetoresistivity. We interpret these findings as a confirmation of a strong interbilayer decoherence and, therefore, the two-dimensional nature of the phase-coherent paths. Under this condition, both components of the conductivity depend on the in-plane phase coherence length ℓ_φ , which changes with field logarithmically, thus producing the corresponding H -dependence of the magnetoresistivities. (2) In high magnetic fields and at low temperatures, both magnetoresistivities become positive and change as γH^2 up to the largest available field of $14 T$. This contribution arises from antiferromagnetic correlations.

II. EXPERIMENTAL DETAILS

Strongly underdoped $YBa_2Cu_3O_x$ ($x = 6.36$ and 6.25) single crystals were grown in gold crucibles using the self-flux method. The oxygen stoichiometry was adjusted by annealing the samples at $500^\circ C$ in a predetermined O_2-N_2 atmosphere [10]. In-plane ρ_{ab} and out-of-plane ρ_c resistivities and the respective magnetoresistivities (MR)

were measured by a multiterminal method on the same single crystal, in magnetic fields H up to 14 T. This allows us to carry out a *quantitative* comparison between in-plane $\Delta\rho_{ab}/\rho_{ab}$ and out-of-plane $\Delta\rho_c/\rho_c$ magnetoresistivities as a function of temperature T and applied magnetic field H . All previous measurements of MR in $YBa_2Cu_3O_x$ reported in the literature were obtained by a four-point method, so that $\Delta\rho_{ab}/\rho_{ab}$ and $\Delta\rho_c/\rho_c$ were measured on different single crystals. Since magnetoresistivity is very small, inevitable variations of stoichiometry, shape, and size of specimens have a large effect on its value and preclude any quantitative analysis of correlations between different components of the magnetoresistivity tensor.

Low contact resistance gold leads were attached using thermally treated silver pads and room temperature silver epoxy. We applied an ac electrical current $I \sim 0.1$ mA through the two leads on the "top" face and measured the two voltage drops on the same (top voltage V_t) and the opposite (bottom voltage V_b) faces of the sample [11]. The two voltages $V_{t,b}$ and their variation with field $\delta V_{t,b}$ were measured using a low-frequency 17 Hz resistance bridge at constant temperature, while sweeping the magnetic field H applied parallel to the c -axis of the single crystal.

The temperature of the sample chamber was kept constant using two temperature sensors (*Pt* thermometer for $T > 100$ K and *Cx* sensor for $T < 100$ K). The temperature change $\delta T(H)$ resulting from the magnetoresistance of the sensors was measured by carefully calibrating them using a capacitance thermometer, which has zero magnetoresistance. The effect of the magnetic field on $V_{t,b}$ was then determined by subtracting the effect of this temperature change from the raw data; i.e.,

$$\Delta V_{t,b}(H) = \delta V_{t,b} - \delta T(H) \frac{dV_{t,b}}{dT}. \quad (1)$$

Unlike in the four-point method, the distribution of the current inside the sample is nonuniform. As a result, the Hall voltage contributes to the field variation of the top and bottom voltages. To first order in magnetoconductivities, appropriate for these measurements,

$$\Delta V_{t,b}(H) = A_{t,b} \Delta\sigma_{xx} + B_{t,b} \Delta\sigma_{zz} + C_{t,b} \sigma_{xy}, \quad (2)$$

where $\Delta\sigma_{xx}$ and $\Delta\sigma_{zz}$ are magnetoconductivities, while σ_{xy} is the off-diagonal component of the conductivity tensor. The coefficients $A_{t,b}$, $B_{t,b}$ and $C_{t,b}$ can be obtained from the solution of Laplace's equation determining the distribution of voltage inside the sample. (Within a linear approximation, these coefficients depend on the zero-field values of the conductivity tensor, which is diagonal.)

The most reliable way to determine the magnetoconductivities $\Delta\sigma_{xx}$ and $\Delta\sigma_{zz}$ from Eq. (2) is to eliminate the contribution of the Hall effect by measuring $\Delta V_{t,b}(H)$ at two opposite polarities $\pm H$ of the applied magnetic field. The even component $\Delta V_{t,b}^+(H) =$

$1/2[\Delta V_{t,b}(H) + \Delta V_{t,b}(-H)]$ determines the magnetoconductivity, while the odd component $\Delta V_{t,b}^-(H) = 1/2[\Delta V_{t,b}(H) - \Delta V_{t,b}(-H)] = C_{t,b} \sigma_{xy}$. The magnetoconductivities were then calculated from $\Delta V_{t,b}^+(H)$ using an algorithm described in [11].

As an example of the raw data, the main panel of Fig. 1 shows the field dependence of ΔV_t of the $x = 6.36$ single crystal, measured at $T = 100$ K, while the inset displays its odd ΔV_t^- and even ΔV_t^+ components. The field dependence of ΔV_t clearly separates into quadratic dependence of ΔV_t^+ and, consequently, of magnetoconductivity, and linear dependence of ΔV_t^- and, hence, Hall conductivity σ_{xy} .

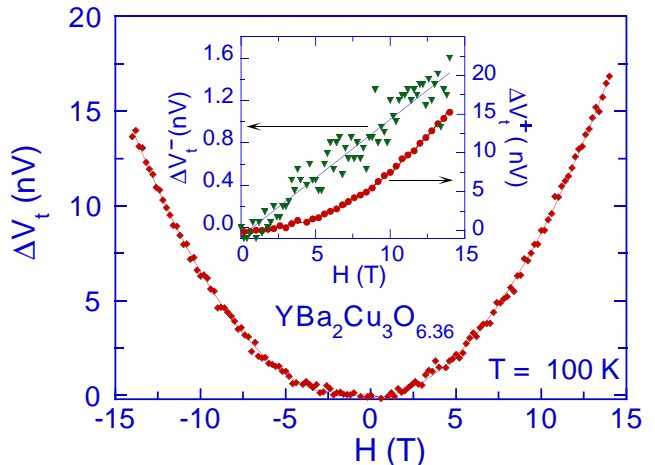


FIG. 1. Main panel: The field H dependence of the top voltage ΔV_t for the $x = 6.36$ single crystal, measured at $T = 100$ K in $H \parallel c$; Inset: odd $\Delta V_t^- = 1/2[\Delta V_t(H) - \Delta V_t(-H)]$ and even $\Delta V_t^+ = 1/2[\Delta V_t(H) + \Delta V_t(-H)]$ components of the top voltage obtained from the data shown in the main panel.

The multiterminal technique has never been used before to measure magnetoconductivities of cuprates. The application of this method to magneto-measurements has subtle, but important, differences with the conventional four-point method. For example, in the multiterminal method one measures magnetoconductivities, while in the conventional four-point method one measures magnetoresistivities. It should be noted that most theoretical approaches to magnetoeffects describe magnetoconductivities rather than magnetoresistivities. Assuming that σ_{xz} and σ_{yz} are negligible, the relationship between magnetoresistivities and magnetoconductivities is given by [12]:

$$\frac{\Delta\rho_{xx}}{\rho_{xx}} = -\frac{\Delta\sigma_{xx}}{\sigma_{xx}} - \frac{\sigma_{xy}^2}{\sigma_{xx}^2}; \quad \frac{\Delta\rho_{zz}}{\rho_{zz}} = -\frac{\Delta\sigma_{zz}}{\sigma_{zz}} \quad (3)$$

Comparing the values of the even and odd components $\Delta V_{t,b}^\pm$, we find that in most cases $\Delta\sigma_{xx} \sim \sigma_{xy}$ and, since both of them are very small, the quadratic term in Eq. (3) is negligible. Therefore, the magnetoresis-

tivities are given directly by magnetoconductivities with inverted sign. The only exception to this case is at very low magnetic fields where $\sigma_{xy} > \Delta\sigma_{xx}$ since $\sigma_{xy} \propto H$ while $\Delta\sigma_{xx} \propto H^2$. Therefore, at very low fields, one needs to know σ_{xy} in order to obtain magnetoresistivity from magnetoconductivity. In this paper, we present all our results in terms of magnetoresistivity obtained from the measured magnetoconductivity according to Eq. (3) where we neglect the quadratic term. This facilitates a direct comparison between our data and already published magnetoresistivity data.

III. MAGNETORESISTIVITY

Figures 2(a) and 2(b) show the T -dependences of the resistivities of $YBa_2Cu_3O_{6.36}$ and $YBa_2Cu_3O_{6.25}$ single crystals, respectively, in zero magnetic field. These single crystals display a diverse T -dependence of resistivities, and antiferromagnetism below $T \approx 40$ K in $x = 6.36$ sample and for all $T < 300$ K in $x = 6.25$ crystal. Coexistence of metallic ρ_{ab} and nonmetallic ρ_c over an extensive temperature range is characteristic of underdoped cuprates. We note that the in-plane resistivity ρ_{ab} is metallic above a certain temperature even in the strongly underdoped samples. The crossover to nonmetallic behavior in ρ_{ab} takes place at progressively higher temperatures in more underdoped samples. For

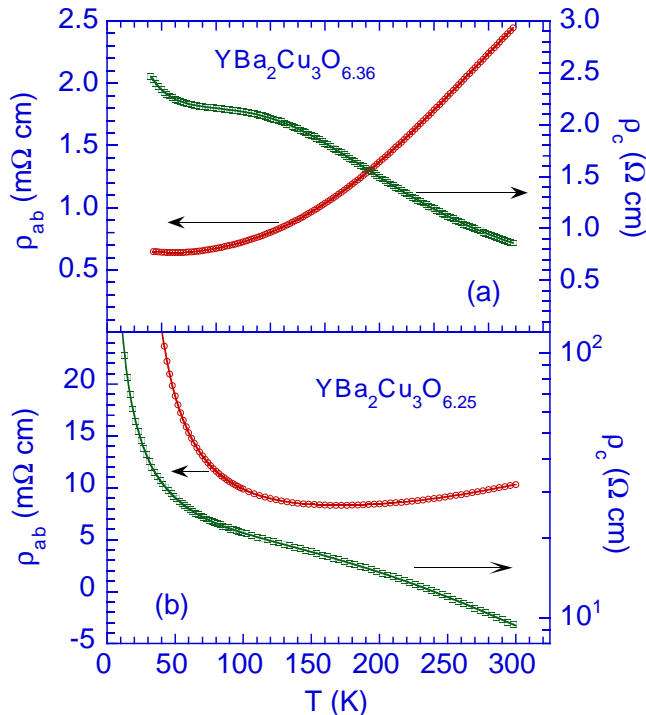


FIG. 2. Temperature T dependence of zero-field in-plane ρ_{ab} and out-of-plane ρ_c resistivities for (a) $YBa_2Cu_3O_{6.36}$, and (b) $YBa_2Cu_3O_{6.25}$.

example, the minimum in ρ_{ab} shifts from ≈ 50 K for the $x = 6.36$ sample to ≈ 175 K for the $x = 6.25$ sample.

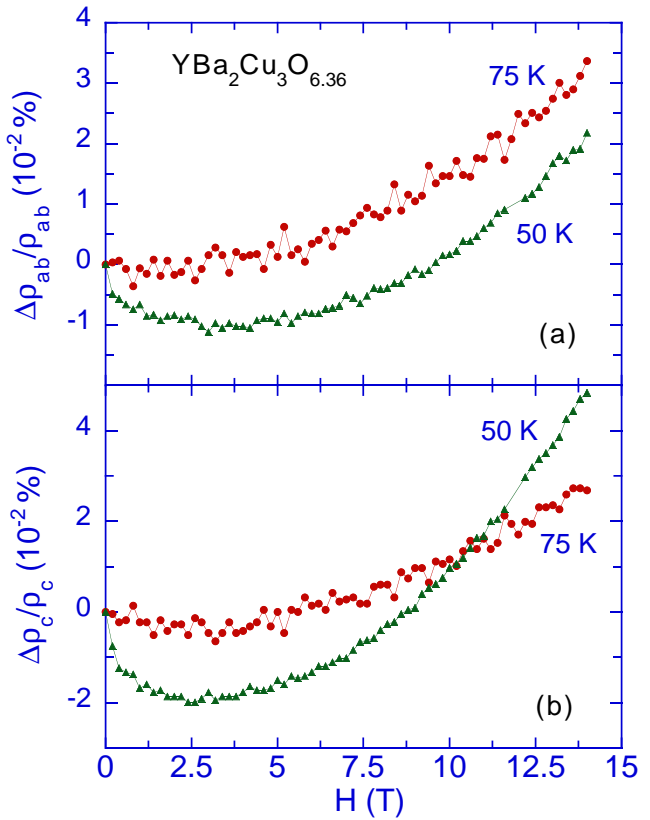


FIG. 3. Field H dependence of magnetoresistivities for $H \parallel c$: (a) $\Delta\rho_{ab}/\rho_{ab}$ and (b) $\Delta\rho_c/\rho_c$ for $YBa_2Cu_3O_{6.36}$ at 50 K and 75 K.

Measurements of the MR tensor on $YBa_2Cu_3O_{6.36}$ at temperatures higher than 75 K showed that the field dependence of both in-plane and out-of-plane MR is quadratic [13]. However, at lower temperatures, the field dependence of the MR tensor becomes non trivial [see Figs. 3(a) and 3(b)]. Namely, at 50 and 75 K, a negative MR component, with a large slope at relatively low fields, is superimposed on a positive quadratic field dependence. Notice that the minimum in $\Delta\rho_c/\rho_c$ is approximately twice the minimum in $\Delta\rho_{ab}/\rho_{ab}$. At higher magnetic fields, MR is positive and changes quadratically with H .

Figures 4(a) and 4(b) display the magnetic field H dependence of MR of the $YBa_2Cu_3O_{6.25}$ single crystal. The same phenomenon as in the previous sample, namely, sharply developing negative MR in low fields which turns into positive quadratic dependence in high fields, is even more pronounced.

The field dependence of MR illustrated in Figs. 3 and 4 can be described for both samples as a sum of two contributions: a negative contribution $Q_i(H)$ where $i = \{c, ab\}$, and a positive quadratic contribution; i.e.,

$$\frac{\Delta\rho_i}{\rho_i} = Q_i(H) + \gamma_i H^2; \quad Q_i(H) < 0; \gamma_i > 0. \quad (4)$$

We examine in more detail the field dependence of the MR components measured at 75 K on $YBa_2Cu_3O_{6.25}$ in Fig. 5 (a). First, we note that the negative contribution to MR is much larger for the out-of-plane component than for the in-plane component; for example, the absolute value of $\Delta\rho_c/\rho_c$ at its minimum is about 7 times the corresponding $\Delta\rho_{ab}/\rho_{ab}$. Second, both $\Delta\rho_c/\rho_c$ and $\Delta\rho_{ab}/\rho_{ab}$ measured in high magnetic fields are well fitted with a parabolic dependence $\gamma_i H^2 - \epsilon_i$, as shown by the solid curves, with $\gamma_c = 1.3 \times 10^{-5} T^{-2}$, $\gamma_{ab} = 6.25 \times 10^{-6} T^{-2}$, $\epsilon_c \approx 0.15\%$, and $\epsilon_{ab} \approx 0.03\%$. We discuss the origin of this quadratic H -dependence at the end of the next Section.

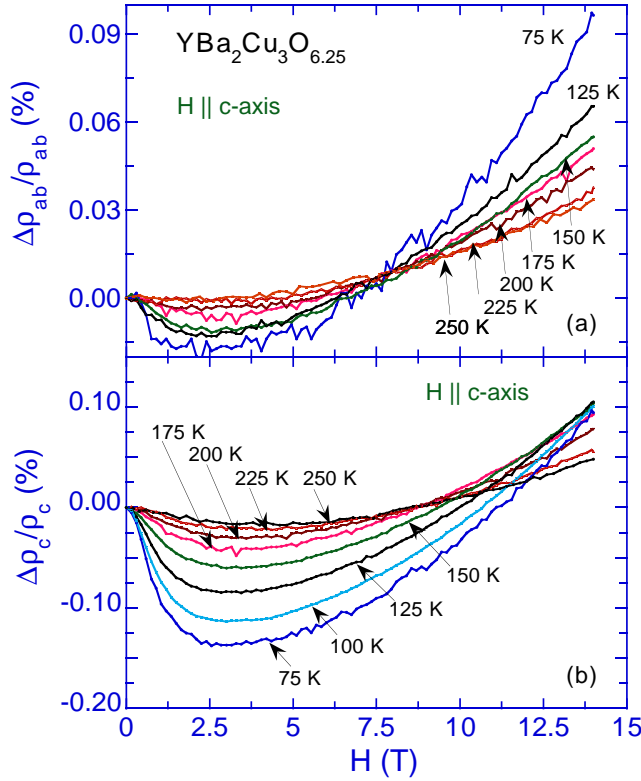


FIG. 4. Field H dependence of magnetoresistivities: (a) $\Delta\rho_{ab}/\rho_{ab}$ and (b) $\Delta\rho_c/\rho_c$ for $YBa_2Cu_3O_{6.25}$.

The field dependence of $Q_i(H)$ in Eq. (4) can be determined by subtracting $\gamma_i H^2$ from the total MR, and is illustrated in the semi-log plot of Fig. 5(b). The straight lines are fits to the data and reveal the logarithmic dependence of $Q_i(H)$ within a certain range of H . The functional dependence of $Q_i(H)$ can be summarized as follows:

$$Q_i \propto \begin{cases} -\epsilon_i \frac{H^2}{H_0^2} & H < H_0 \\ -\epsilon_i \frac{\ln(H/H_0)}{\ln(H_1/H_0)} & H_0 < H < H_1 \\ -\epsilon_i & H > H_1 \end{cases} \quad (5)$$

The most interesting part is the logarithmic dependence,

covering almost a decade of H . The value of the parameter H_0 is determined by the intercept of the straight line according to Eq. (5). For $H > H_1 \approx 4 T$, $Q_i(H)$ saturates at the value of ϵ_i obtained earlier by the parabolic fit in Fig. 5(a). The $\ln(H_1/H_0)$ in the denominator of Eq. (5) is required to match the interpolations of $Q_i(H)$ at $H_0 < H < H_1$ and $H > H_1$.

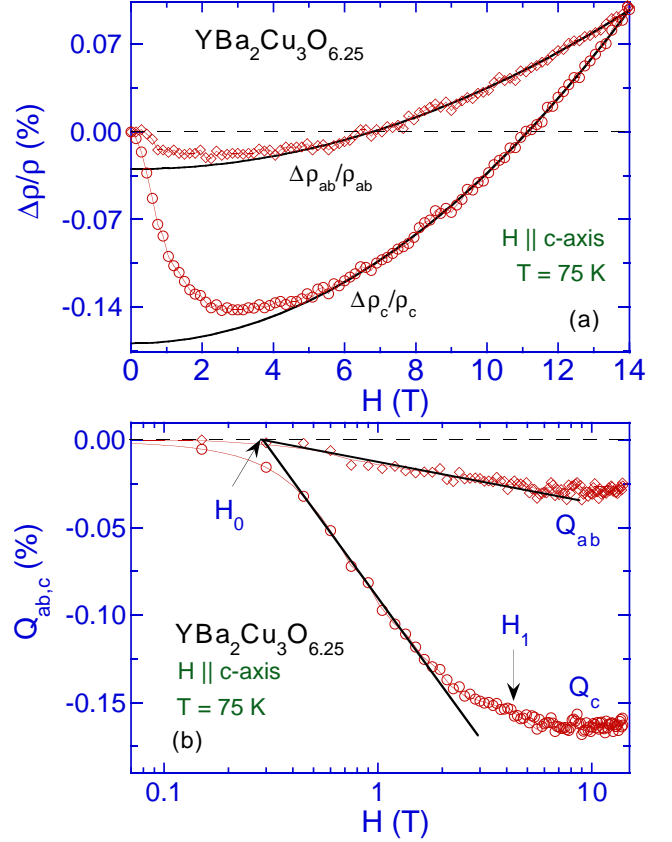


FIG. 5. (a) Magnetoresistivities $\Delta\rho_c/\rho_c$ and $\Delta\rho_{ab}/\rho_{ab}$ for $YBa_2Cu_3O_{6.25}$ at $T = 75 K$ in magnetic fields $H||c$. The solid lines represent quadratic fits $\gamma_i H^2 - \epsilon_i$ ($i = \{c, ab\}$). (b) Orbital component of magnetoresistivity $Q_i = \Delta\rho_i/\rho_i - \gamma_i H^2$ plotted vs logarithm of field. The straight lines are guides to the eye corresponding to the logarithmic dependence given by Eq. (5). The crossover fields H_0 and H_1 are indicated.

The negative contribution to the in-plane MR is smaller and, therefore, the data are noisier, but a similar procedure of fitting the high field regime data with a parabolic dependence yields $Q_{ab}(H)$ with approximately the same H -dependence as $Q_c(H)$; i.e., $Q_c(H)/Q_{ab}(H) \approx const = 7$.

IV. DISCUSSION

The most intriguing observation that emerges from the data presented above (Figs. 3 and 4) is the presence of a negative MR component in low fields [given by $Q_i(H)$ in Eq. (4)], especially pronounced in $\Delta\rho_c/\rho_c$, which exhibits

at the lowest accessible temperatures a logarithmic H -dependence. This negative MR is superimposed on a positive quadratic background [$\gamma_i H^2$ in Eq. (4)], which is due to antiferromagnetic ordering [14]. Below, we show that the low field features of MR are direct consequences of interlayer incoherence.

Our approach is based on the understanding that strongly underdoped layered crystals like $YBa_2Cu_3O_x$ are characterized by incoherent out-of-plane transport. This was shown in optical measurements of the conductivity on underdoped $YBa_2Cu_3O_x$ [3]. In incoherent crystals, the value of the out-of-plane coherence length $\ell_{\varphi,c}$ is T -independent, equal to its minimum possible value. Since the coherence length of electron wave functions in a crystal cannot be smaller than the size of the atomic orbitals that overlap over the interbilayer distance, the minimum possible value of $\ell_{\varphi,c}$ is the interbilayer distance; i.e., $\ell_{\varphi,c} = \ell_0 = 11.7\text{\AA}$. Thus, a fundamental property of fully incoherent crystals is that $\ell_{\varphi,c}$ does not change with temperature or magnetic field. Therefore, the only length scale which determines the dissipation and can change with temperature or applied magnetic field is the in-plane phase coherence length ℓ_{φ} . (Hereafter, we assume for brevity that the planes are isotropic and omit the subscript ab .) Under these conditions, both conductivities depend only on the variable ℓ_{φ} [$\sigma_{ab}(\ell_{\varphi})$ and $\sigma_c(\ell_{\varphi})$], so that their temperature and field dependences come from that of ℓ_{φ} . (An instructive discussion regarding the dependence of conductivity on the spatial length scale of inelastic scattering processes is presented in [8]).

The immediate consequence is a correlation between the magnetoconductivities and the field variation of the in-plane coherence length at constant T :

$$\frac{\Delta\sigma_{ab}(H)}{\sigma_{ab}} = \kappa_{ab} \frac{\Delta\ell_{\varphi}(H)}{\ell_{\varphi}}; \quad \frac{\Delta\sigma_c(H)}{\sigma_c} = \kappa_c \frac{\Delta\ell_{\varphi}(H)}{\ell_{\varphi}}. \quad (6)$$

where $\kappa_i \equiv d \ln \sigma_i / d \ln \ell_{\varphi}$ ($i = \{ab, c\}$).

The coefficients κ_i are dimensionless numbers of the order of unity. Their sign determines the type of electrical conduction (metallic or nonmetallic); i.e., if $\kappa_i > 0$, then $\partial\sigma_i/\partial T < 0$ and the conduction is metallic, while if $\kappa_i < 0$, then $\partial\sigma_i/\partial T > 0$ and the conduction is nonmetallic [15]. It is important to remember that in Eq. (6) and hereafter, $\Delta\sigma_{ab}/\sigma_{ab}$ and $\Delta\sigma_c/\sigma_c$ are the "orbital" contributions to magnetoconductivity also denoted as Q_i in Eq. (4).

According to Eq. (6), the sign of the MR tensor is determined by the sign of κ_i and by the effect of the magnetic field on ℓ_{φ} . It is known [6], and in the Appendix shown in more detail, that the magnetic field decreases the phase coherence length due to its effect on self-intersecting trajectories, so that $\Delta\ell_{\varphi}(H) < 0$ in a weak field. The sign of κ_i can be inferred from the T -dependence of the resistivity. Specifically, for

$YBa_2Cu_3O_{6.25}$, $\kappa_{c,ab}(T) < 0$ for $T < 175\text{ K}$ since both ρ_c and ρ_{ab} are nonmetallic [see Figs. 2(a) and 2(b)]. Then, according to Eq. (6), both magnetoconductivity components are positive (MR, correspondingly, are negative) for $T < 175\text{ K}$, as indeed is the case [see Fig. 4]. By applying the same reasoning to the $YBa_2Cu_3O_{6.36}$ sample, one concludes that $\Delta\rho_c/\rho_c$ should be negative, while $\Delta\rho_{ab}/\rho_{ab}$ should be practically zero at 75 K and should become negative for $T \leq 50\text{ K}$, where ρ_{ab} turns nonmetallic as well. This is consistent with the low field data of Fig. 3.

Also, according to Eq. (6), the field dependence of both MR is the same, determined by that of $\Delta\ell_{\varphi}(H)$. Therefore, their ratio should be a constant, given by the ratio of the corresponding κ_i ; i.e.,

$$\frac{\Delta(\ln \sigma_c)}{\Delta(\ln \sigma_{ab})} = \frac{\kappa_c}{\kappa_{ab}}. \quad (7)$$

As discussed in Refs. [16,17], in incoherent crystals $\sigma_c(\ell_{\varphi}) \propto \sigma_{ab}(\ell_{\varphi})/\ell_{\varphi}^2$. As a result, $\kappa_c = \kappa_{ab} - 2$. Therefore, when κ_{ab} is negative (as is the case with our crystals at low temperatures), the absolute value of $\Delta(\ln \sigma_c)$ is greater than that of $\Delta(\ln \sigma_{ab})$, namely:

$$\frac{\Delta(\ln \sigma_c)}{\Delta(\ln \sigma_{ab})} = \frac{|\kappa_{ab}| + 2}{|\kappa_{ab}|}. \quad (8)$$

In other words, when the T -dependence of both conductivities is nonmetallic, the out-of-plane conductivity depends stronger on the phase coherence length, and the respective MR is greater by a constant factor.

This conclusion is, indeed, supported by the experimental data. The ratio of the magnetoresistivities is a constant factor which can be estimated, for example, from Fig. 5(b). Namely, for $YBa_2Cu_3O_{6.25}$ at $T = 75\text{ K}$, Q_c is about seven times greater than Q_{ab} . From Eq. (8), we estimate $\kappa_{ab} \approx -0.33$.

We turn now our attention to the specific field dependence of the magnetoresistivities. The logarithmic field dependence of Q at low temperatures and in relatively small magnetic fields indicates 2D quantum interference [6,8]. This effect is due to the presence of self-intersecting trajectories along which electrons can traverse the loop in opposite directions [6,8]. A small applied magnetic field gradually destroys the quantum interference, which induces a variation in the phase coherence length and, therefore, a variation in the conductivity.

The self-intersecting trajectories constitute a small fraction of the total number of phase coherent trajectories of a given length. The great majority of the phase coherent trajectories (trajectories over which the phase changes predictably and, therefore, no irreversible processes are involved) are not self-intersecting.

As Fig. 2 shows, both resistivities change strongly with temperature and, therefore, their magnitude and T -dependence are determined by the contribution of the

majority, non-intersecting trajectories. The small, temperature dependent corrections to conductivities (in zero field) due to self-intersecting trajectories, known as corrections due to weak localization, can only be observed when the main contribution to conductivity which is due to non-intersecting paths saturates (regime of residual resistivity). Our samples are not in this regime. Therefore, the contribution of the trajectories with loops to the T-dependence of both conductivities is negligible in our samples and $\sigma_{ab}(T)$ and $\sigma_c(T)$ do not reflect the characteristic $\ln T$ (in 2D) or $T^{1/2} - T^{1/3}$ (in 3D) dependence due to quantum interference, which is usually the subject of discussion in the literature.

On the other hand, the magnetoconductivity produced by a *weak* magnetic field is due to self-intersecting trajectories because all the other (conventional) contributions to magnetoconductivity are still negligible. Therefore, the magnetoconductivity caused by the effect of the field on the self-intersecting trajectories can be experimentally identified.

In order to determine the field dependence of both magnetoconductivities, we need to evaluate the magnetic field variation of the coherence length $[\Delta\ell_\varphi(H)/\ell_\varphi]$. A semi-quantitative derivation of this dependence is given in the Appendix, with the following results:

$$\frac{\Delta\ell_\varphi}{\ell_\varphi} \propto \begin{cases} -\eta H^2/H_0^2 & H < H_0 \\ -\eta \frac{\ln(H/H_0)}{\ln(H_1/H_0)} & H_0 < H < H_1 \\ -\eta & H > H_1 \end{cases} \quad (9)$$

Here η is a small number determined by the relative weight of the number of the self-intersecting trajectories with respect to that of the majority nonintersecting trajectories. The lower crossover field H_0 is determined by the condition that the field flux through the largest loops along the phase coherent trajectories is approximately equal to the flux quantum $\phi_0 = 2 \times 10^{-7} Oe \text{ cm}^2$; namely $H_0 \sim \phi_0/\ell_\varphi^2$. The upper crossover field H_1 is determined by the similar condition that the field flux is of the order of ϕ_0 through the smallest possible loops (of the order of the elastic mean free path ℓ_{el}); i.e., $H_1 \sim \phi_0/\ell_{el}^2$. For $H > H_1$, no trajectory with loops contributes to the value of the phase coherence length. Hence, $\Delta\ell_\varphi$ saturates.

From Eqs. (6) and (9) follows Eq. (5) with $\epsilon_i = -\eta \kappa_i$. The nontrivial logarithmic field dependence appears only when there is a significant field range between H_0 and H_1 . This requires the phase coherence length to be substantially greater than the elastic mean free path, which means a well developed diffusive regime. Therefore, the magnetoeffects due to self-intersecting trajectories are more pronounced in stronger underdoped samples. For $YBa_2Cu_3O_{6.25}$ at $T = 75 \text{ K}$ [see Fig. 5(b)], we estimate that $\epsilon_c \approx 0.15\%$, $H_0 \sim 0.3 \text{ T}$ which corresponds to $\ell_\varphi \sim 10^3 \text{ \AA}$, and $H_1 \sim 4 \text{ T}$ ($\ell_{el} \sim 270 \text{ \AA}$). For $H > 4 \text{ T}$, the contribution of quantum interference to magnetoconductivities saturates and other types of contributions to

MR become dominant, as discussed below.

Experimentally, one can relatively easily distinguish between the cases of two-dimensional and three-dimensional phase coherent trajectories. First, the magnetoeffect of self-intersecting trajectories is substantially greater in 2D, because of the greater probability of a 2D trajectory to form a large loop ($\eta \sim \lambda/\ell_{el}$ in 2D and $\eta \sim \lambda^2/\ell_{el}^2$ in 3D, see the Appendix). Therefore, in this case, the effect becomes pronounced and observable at relatively high temperatures. Second, the logarithmic H dependence can be distinguished from $H^{1/2}$ rather clearly even for only one decade in H . These features observed in MR would point to the 2D nature of the phase coherent trajectories. The two manifested together, as is the case with our MR data of $YBa_2Cu_3O_x$ shown above, make this conclusion very compelling. It should be noted that the "three dimensional" $H^{1/2}$ dependence of MR in manganites was reported recently by Qing'An Li, Gray, and Mitchell [18].

Finally, we discuss briefly the origin of the positive contribution that changes as $\gamma_i H^2$ and becomes dominant at applied magnetic fields larger than 4 T (see Figs. 3 and 4). A similar type of MR was reported by other groups as well [14], and it was associated with the antiferromagnetic fluctuations and antiferromagnetic ordering. Indeed, $YBa_2Cu_3O_{6.25}$ is antiferromagnetic for all temperatures below room temperature, while $YBa_2Cu_3O_{6.36}$ is antiferromagnetic for $T \leq 40 \text{ K}$. In high magnetic fields, the contribution of the AF correlations to MR dominates the smaller contribution of the self-intersecting trajectories. At sufficiently low temperatures, these two contributions can be clearly separated as illustrated in Figs. 5(a) and 5(b).

V. SUMMARY

We present magnetoresistivity data for two strongly underdoped single crystals of $YBa_2Cu_3O_x$ with $x = 6.36$ and 6.25 . Both in-plane $\Delta\rho_{ab}$ and out-of-plane $\Delta\rho_c$ magnetoresistivities MR were measured simultaneously on the same single crystal using a multiterminal method. This permits a direct comparison between their temperature and field dependences.

The most interesting observation is a negative MR in low applied magnetic fields. This low field contribution is characterized by two important features: First, the effect is strong and, therefore, is pronounced even at relatively high temperatures (75 K and higher). Second, the field dependence is consistent with $\ln(H)$, rather than $H^{1/2}$. These features point towards the two dimensional nature of the phase coherence in these crystals; namely, the phase-coherent volume contains only one or two neighboring bilayers, while the coherence length along the planes is orders of magnitude greater than the size of the unit cell.

We attribute the second contribution to MR, which changes quadratically with field up to $H = 14 T$, to the effect of H on the AF correlations. This positive contribution dominates at fields above $4 T$ and induces a change in the sign of the total MR for both components of the magnetoresistivity.

VI. APPENDIX

To determine the effect of the magnetic field on self-intersecting phase coherent trajectories, and the resultant effect on the phase coherence length, we use the qualitative approach described in [6,8]. The coherent trajectories consist of two groups. The great majority of them are not self-intersecting and they determine the value and the temperature dependence of the phase coherence length and, consequently, of the conductivities. A much smaller fraction of the coherent trajectories have loops and exhibit the interference effect.

We begin our estimate by defining the phase coherence length in zero magnetic field $\ell_\varphi(0)$ as the mean square average distance in the x-direction that an electron travels while retaining its phase memory (i.e., without encountering dephasing inelastic collisions):

$$\ell_\varphi^2(0) = \int_0^\infty x^2 [(1-\eta)P_0(x) + \eta P_{si}(x)] dx. \quad (10)$$

Here $P_0(x)$ [$P_{si}(x)$] is the probability that the phase coherence is retained between points A and B separated by a distance x , when all trajectories without [with] self-intersections are counted. Both probabilities are normalized to unity. The small number $\eta \ll 1$ reflects the relative weight of self-intersecting trajectories. We also introduce $p(x, \mathcal{A})$ as the probability density that a self-intersecting, coherent trajectory (in zero field) has a loop of area \mathcal{A} , subject to the normalization condition:

$$\int_{\pi\ell_{el}^2}^{\pi x^2} p(x, \mathcal{A}) d\mathcal{A} = P_{si}(x). \quad (11)$$

Here, the smallest possible area of the loop is determined by the elastic mean free path ℓ_{el} , and the largest possible loop is determined by the distance x between A and B .

Along self-intersecting trajectories, an electron can traverse the loop in opposite directions with no phase difference between the respective amplitudes. An applied magnetic field, however, introduces a phase difference $\varphi_H = 2\pi\phi/\phi_0$ between the two alternative routes along the same trajectory. Here $\phi = \mathcal{A}H$ is the magnetic field flux through the loop, \mathcal{A} is the area of the loop normal to the field, and $\phi_0 = 2 \times 10^{-7} Oe \text{ cm}^2$ is the flux quantum. As a result, when an electron arrives at point B , following a self-intersecting route, its phase is unpredictable, and varies by $\varphi_H \geq \pi$ if the corresponding trajectory has

a loop with area $\mathcal{A} \geq \phi_0/2H$. Therefore, such a trajectory is no longer phase coherent and does not contribute to the average given by Eq. (10). This is the mechanism by which a weak field changes the coherence length and, respectively, the conductivities.

We give a rough estimate of $\Delta\ell_\varphi(H)$ by considering that all self-intersecting trajectories with loop areas $\mathcal{A} \geq \phi_0/2H$ do not contribute to the average in Eq. (10), while those with $\mathcal{A} < \phi_0/2H$ still do. The phase coherence length in a magnetic field is then given by:

$$\ell_\varphi^2(H) = \int_0^\infty x^2 dx \left[(1-\eta)P_0(x) + \eta \int_{\pi\ell_{el}^2}^{\pi\ell_H^2} p(x, \mathcal{A}) d\mathcal{A} \right], \quad (12)$$

where the magnetic length $\ell_H = (\hbar c/2eH)^{1/2}$ is determined by the condition $\pi\ell_H^2 = \phi_0/2H$.

Taking into account Eqs. (10) and (11) and the small value of η , we obtain from Eq. (12):

$$\frac{2\Delta\ell_\varphi(H)}{\ell_\varphi} \approx -\eta \frac{\int_{\ell_H}^\infty x^2 dx \int_{\pi\ell_H^2}^{\pi x^2} p(x, \mathcal{A}) d\mathcal{A}}{\int_0^\infty x^2 P_0(x) dx}. \quad (13)$$

Thus, the *decrease* of the phase coherence length $\Delta\ell_\varphi(H)$ is proportional to the weight of excluded self-intersecting trajectories, namely, those with loop areas $\mathcal{A} \geq \pi\ell_H^2$. The lower limit of integration in x is ℓ_H because the trajectories with a coherent distance $x \leq \ell_H$ cannot have loops with area $\mathcal{A} \geq \pi\ell_H^2$ and, therefore, are not part of the excluded self-intersecting trajectories.

Next we find the expression for $p(x, \mathcal{A})$ using the diffusive approximation [8]. Since phase-coherent trajectories are two-dimensional (we discuss here incoherent crystals), the probability to find an electron at a point \vec{r} from its starting origin at $t = 0$, is $W(\vec{r})d^2r \propto \exp(-\vec{r}^2/4Dt)d^2r/4Dt$, where D is the diffusion coefficient. The trajectory intersects itself between the times t and $t + dt$ if it enters the area $\lambda v dt$ around the origin. Here λ is the de Broglie wavelength (the trajectory is viewed as a tape of width λ , rather than a line). The probability of return, and, consequently, the probability to form a loop is given by $p(t)dt \propto W(0)\lambda v dt \propto \lambda v dt/Dt$. Since the area of the loop is proportional to the average distance from the origin, $\mathcal{A} \propto \langle \vec{r}^2 \rangle \propto Dt$, and $d\mathcal{A} \propto Ddt$, the probability of a loop with area between \mathcal{A} and $\mathcal{A} + d\mathcal{A}$ is given by $(\lambda v/D)d\mathcal{A}/\mathcal{A}$. Thus, the probability that a 2D trajectory has a loop of area \mathcal{A} scales as $1/\mathcal{A}$.

The prefactor $\lambda v/D$ determines the overall probability of self-intersecting trajectories and gives the number η , which we introduced "by hand" earlier: $\eta \sim \lambda v/D \sim \lambda/\ell_{el}$, because $D \sim v\ell_{el}$. Assuming $\lambda \sim 2 - 3 \text{ \AA}$ and $\ell_{el} \sim 200 - 300 \text{ \AA}$, which is a reasonable estimate given the density of charge carriers, we obtain $\eta \sim 0.01$. It means that the maximum effect of removing self-intersecting trajectories from the average in Eq. (13) reduces ℓ_φ by about one percent. Other numerical factors

also absorbed in η can reduce it further. This correlates with the maximum value of the negative MR in Fig. 5(b) of the order of 0.1%.

Since the diffusive motion has no memory, having a loop does not affect the statistical properties of the rest of the trajectory. Therefore, the probability density $p(x, \mathcal{A})d\mathcal{A}$ can be roughly estimated as:

$$p(x, \mathcal{A})d\mathcal{A} \approx \frac{P_{si}(x)}{\ln(x^2/\ell_{el}^2)} \frac{d\mathcal{A}}{\mathcal{A}}, \quad (14)$$

where the logarithm in the denominator is the normalization factor due to Eq. (11). Now the integral in (13) becomes:

$$\int_{\ell_H}^{\infty} x^2 dx \int_{\pi\ell_H^2}^{\pi x^2} p(x, \mathcal{A})d\mathcal{A} = \int_{\ell_H}^{\infty} x^2 P_{si}(x) \frac{\ln(x^2/\ell_H^2)}{\ln(x^2/\ell_{el}^2)} dx. \quad (15)$$

The characteristic logarithmic field dependence of this integral appears when ℓ_H^2 decreases below the value of ℓ_{φ}^2 . This is equivalent to the condition that the field flux through the largest loops along the phase coherent trajectories is approximately equal to $\phi_0/2$; hence, the characteristic field $H_0 = \phi_0/2\pi\ell_{\varphi}^2$. As ℓ_{φ} increases with decreasing temperature, the onset field H_0 can become very small and the MR due to the interference effect manifests itself when all the other sources of MR are negligible. The upper crossover field is defined by the condition that the field flux is $\phi_0/2$ through the smallest loops with the area of the order of $\pi\ell_{el}^2$; hence $H_1 = \phi_0/2\pi\ell_{el}^2$. The upper field does not change with temperature, while the lower field H_0 decreases with decreasing T . Therefore, this effect is observable at sufficiently low temperatures when $H_0 < H < H_1$ or, equivalently, $\ell_{\varphi}^2 > \ell_H^2 > \ell_{el}^2$.

In this regime, the integral (15) can be easily estimated because the logarithms are slowly changing functions and they can be taken at the value $x \approx \ell_{\varphi}$, which corresponds to the maximum in $x^2 P_{si}(x)$. Other contributions to this integral are negligible in comparison with the logarithmic increase $\sim \ln(\ell_{\varphi}^2/\ell_H^2) = \ln(H/H_0)$. Correspondingly, the logarithm in the denominator of Eq. (15) becomes $\ln(\ell_{\varphi}^2/\ell_{el}^2) = \ln(H_1/H_0)$. In this regime, the denominator in Eq. (13), $\int_0^{\infty} x^2 P_0(x)dx \sim \int_0^{\infty} x^2 P_{si}(x)dx \approx \ell_{\varphi}^2$, and we get Eq. (9), with all numerical factors absorbed in η . Hence, according to Eq. (6), both conductivities have the logarithmic field dependence. For $H > H_1$, the integral (15), hence, Eq. (13) saturates since no self-intersecting trajectories contribute to the average (12).

It is important to underline that the transport in these crystals is obviously three-dimensional, but the phase coherence is two-dimensional, meaning that the distribution of the area of the loops along phase coherent trajectories scales as $1/\mathcal{A}$, leading to the logarithmic field dependence of $\Delta\ell_{\varphi}(H)$ and both magnetoconductivities. This result remains valid even when the coherence is established between two neighboring bilayers. As long as

$\ell_{\varphi,c} \sim \ell_0 \ll \ell_{\varphi,ab}$, the distribution of loop areas is close to $1/\mathcal{A}$.

Truly 3D phase coherent trajectories requires $\ell_{\varphi,c} \gg \ell_0$. Then, a similar analysis [8] shows that the distribution of the loop areas is $d\mathcal{A}/\mathcal{A}^{3/2}$ and $\eta \sim \lambda^2/\ell_{el}^2$. Then, in the regime $H_0 \ll H \ll H_1$, Eq. (A) gives

$$\frac{\Delta\ell_{\varphi}(H)}{\ell_{\varphi}} \sim -\frac{\lambda^2 \ell_{el}}{\ell_{el}^2 \ell_H} \sim -\frac{\lambda^2}{\ell_{el}^2} \left(\frac{H}{H_1}\right)^{1/2} \quad (16)$$

This research was supported by the National Science Foundation under Grant No. DMR-9801990 at KSU and the US Department of Energy under Contract No. W-31-109-ENG-38 at ANL.

-
- [1] P. W. Anderson, *The Theory of Superconductivity in the High- T_c Cuprates*, Princeton University Press, page 36 (1997).
 - [2] M. J. Graf, D. Rainer, and J. A. Sauls, *Phys. Rev. B* **47**, 12089 (1993).
 - [3] D. N. Basov, S. I. Woods, A. S. Katz, E. J. Singley, R. C. Dynes, M. Xu, D. G. Hinks, C. C. Homes, and M. Strongin, *Science* **283**, 49 (1999).
 - [4] Y. Y. Zha, S. L. Cooper, and D. Pines, *Phys. Rev. B* **53**, 8253 (1996).
 - [5] A. A. Abrikosov, *Phys. Rev. B* **55**, 11735 (1997).
 - [6] B. L. Altshuler, A. G. Aronov, D. E. Khmel'nitskii, and A. I. Larkin, *Quantum Theory of Solids*, Ed. by I. M. Lifshits, Mir, Moscow (1982).
 - [7] P. A. Lee and T.V. Ramakrishnan, *Rev. Mod. Phys.* **57**, 287 (1985).
 - [8] A. A. Abrikosov, *Fundamentals of the Theory of Metals*, North-Holland (1988).
 - [9] Y. Kawaguchi and S. Kawagi, *J. Phys. Soc. Japan*, **42**, 699 (1980).
 - [10] B. W. Veal, H. You, A. P. Paulikas, H. Shi, Y. Fang, and J. W. Downey, *Phys. Rev. B* **42**, 4770 (1990).
 - [11] C.N. Jiang, A.R. Baldwin, G.A. Levin, T. Stein, C.C. Almasan, D.A. Gajewski, S.H. Han, and M.B. Maple, *Phys. Rev. B* **55**, R3390 (1997).
 - [12] A. B. Pippard, *Magnetoresistance in Metals*, Cambridge University Press, (1989).
 - [13] E. Cimpoiasu, G. A. Levin, C. C. Almasan, Hong Zheng, and B. W. Veal, *Physica C* **341**, 1879 (2000).
 - [14] A. N. Lavrov, Y. Ando, K. Segawa, and J. Takeya, *Phys. Rev. Lett.* **83**, 1419 (1999).
 - [15] Indeed, since in-plane σ_{ab} and out-of-plane σ_c conductivities are solely functions of ℓ_{φ} , the following equation holds:

$$\frac{\partial \ln \sigma_{c,ab}}{\partial T} = \kappa_{c,ab} \frac{\partial \ln \ell_{\varphi}}{\partial T}. \quad (17)$$

Since the coherence length always decreases with increasing temperature, i. e. $\partial\ell_{\varphi}/\partial T < 0$, the sign of κ_i determines the sign of $\partial\sigma_i/\partial T$, hence the type of conduction.

- [16] G. A. Levin and C. C. Almasan, cond-mat/9907306.

- [17] C. C. Almasan, E. Cimpoiasu, G. A. Levin, H. Zheng, A. P. Paulikas, and B. W. Veal, *J. Low. Temp. Phys.* **117**, 1307 (1999); cond-mat/9908233.
- [18] Qing'An Li, K. E. Gray, and J. F. Mitchell (unpublished).